Appl Phys B (2008) 93: 245–249
DOI 10.1007/s00340-008-3156-6

Applied Physics B
Lasers and Optics

Na-irradiated alpha-quartz: chemical epitaxy and luminescence

S. Gąsiorek · K.P. Lieb · P.K. Sahoo · J. Keinonen

Received: 10 June 2008 / Published online: 27 August 2008

Abstract Doping of α-quartz by ion implantation leads to amorphization even at low fluences, but subsequent annealing in air or oxygen can restore the crystalline order (chemical epitaxy). Here we report on measurements of RBS channeling and cathodoluminescence (CL) spectra during chemical epitaxy of α-quartz irradiated with 50-keV Na-ions and annealed in $^{18}O_2$-gas. In particular, the variation of the damage profile and CL spectra (the latter taken at 10 K and 300 K) as functions of the ion fluence will be discussed. The CL spectra at 10 K are dominated by a 2.90-eV band and differ greatly from the ones taken at 300 K; the intensity of this band increases strongly with the Na ion fluence. Some conclusions concerning the underlying photoactive defect structures will be drawn.

PACS 61.80.Jh · 81.15.Np · 42.70.Ce

1 Introduction

Motivated by the rapid progress in designing optoelectronic materials and devices, the amorphous and crystalline forms of silicon dioxide doped with photoactive ions or nanoparticles have been investigated in much detail [1–3]. Since doping quartz by ion beam implantation disturbs or even destroys its crystalline long-range order, many attempts at solid-phase epitaxial regrowth of the damaged/amorphized layers by means of *dynamic*, *chemical*, or *laser-annealing* epitaxy have been made [4–8]. Alkali-ion implantation of α-quartz followed by thermal annealing in air or oxygen, a process called *chemical epitaxy*, indeed provides complete epitaxy around 1100 K [4, 6–11]. The recrystallization is accompanied by alkali out-diffusion and oxygen exchange between the annealing gas and the matrix, as verified by Rutherford backscattering channeling spectroscopy (RBS-C) and time-of-flight elastic recoil detection analysis (TOF-ERDA) after annealing the samples in $^{18}O_2$ tracer gas [4, 6–8, 10, 11].

The current study focuses on the interplay between the cathodoluminescence (CL) and chemical epitaxy in Na-ion implanted α-quartz. For Na-ion fluences of 2.5×10^{16} and 5×10^{16} ions/cm^2, full recrystallization occurs around 1150 K [9]. Recent results on CL emission in this and similar systems at room temperature gave some insight in the nature of the photoactive defects [9–11]. The present investigation aims at studying the epitaxial growth and CL emission as functions of the implanted Na-ion fluence at the fixed annealing temperature of 1123 K. In particular CL emission spectra were investigated at 10 K sample temperature, to be compared with those previously measured at room temperature [9]. These are to our knowledge the first low-temperature CL measurements reported for the process of chemical epitaxy of ion-irradiated α-quartz.

2 Experiments

Samples of single-crystalline (0001) synthetic α-quartz, $10 \times 10 \times 1$ mm^3 in size, were irradiated at liquid-nitrogen

S. Gąsiorek · K.P. Lieb (✉) · P.K. Sahoo · J. Keinonen
II. Physikalisches Institut, Georg-August-Universität Göttingen,
Friedrich-Hund-Platz 1, 37077 Göttingen, Germany
e-mail: plieb@gwdg.de
Fax: +49-551-394493

P.K. Sahoo
Paul Scherrer Institut, 5232 Villigen PSI, Switzerland

J. Keinonen
University of Helsinki, 00014 Helsinki, Finland

temperature with 50-keV Na^+-ions to fluences of 10^{14}–10^{17} ions/cm^2 at a beam current of 1.5 μA. All the ion implantations were performed at normal incidence by means of the Göttingen implanter IONAS [12] and an electric xy sweeping system. According to calculations with the SRIM2000 code [13], the ions have a mean projected ion range of 110 nm when using the atomic density of 6.45×10^{22} atoms/cm^3 in amorphous SiO_2. To study chemical epitaxy, the amorphized samples were annealed for 1 h in $^{18}O_2$ gas at the fixed temperature of 1123 K. Each sample was enclosed inside a quartz ampoule. RBS-C by means of a 15-nA beam of α-particles at 0.9 MeV beam energy provided the information on the radiation damage profiles in the matrix and the degree of recrystallization.

The CL spectra were recorded at either 10 K or 300 K sample temperature using a 5-keV 2-μA electron beam (1 W/cm^2), a Czerny-Turner spectrograph (Jobin Yvon 1000M), and a Hamamatsu R928 photomultiplier. For taking the 10-K data, the sample was attached to a closed-cycle helium cryostate. The CL spectra were collected for an integration time of 700 s in steps of 1 nm/s in the wavelength range between 200 and 700 nm using a grating of 1 200 lines/mm. They were de-convoluted with up to five Gaussian-shaped sub-bands; their emission intensities were corrected for the instrument response function, which was calibrated using a standard halogen lamp. Further details can be found in [9].

3 Results and discussion

3.1 Epitaxy

The RBS-C spectra illustrated in Fig. 1 indicate that for Na-ion fluences increasing from 1×10^{14}/cm^2 to 1×10^{17}/cm^2,

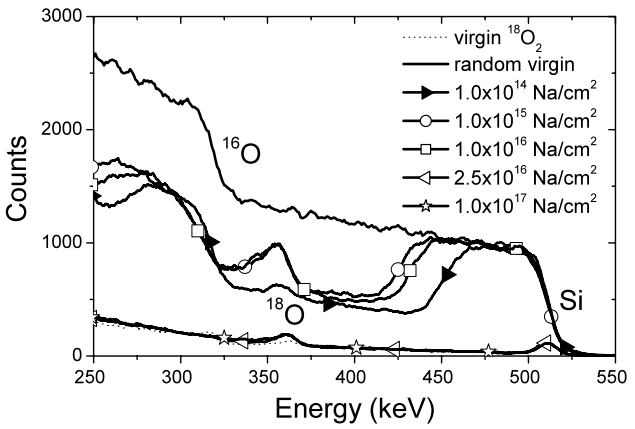

Fig. 1 RBS-channeling spectra of quartz, virgin and random non-irradiated, after irradiation with 50-keV Na ions and 1-h annealing in $^{18}O_2$ gas at 1123 K. Note the progressing epitaxy of the SiO_2 matrix for increasing Na-ion fluence

the amorphized layer recrystallizes progressively during the 1-h annealing at 1123 K. For the lowest fluence, there remains a 200-nm thick amorphized layer, which increases to some 300 nm thickness for fluences of 1×10^{15} and 1×10^{16} Na-ions/cm^2. Starting at a fluence of 2.5×10^{16} Na-ions/cm^2, a recrystallized layer evolves showing little differences relative to the virgin sample. When further increasing the ion fluence, the very low degree of damage remains essentially unchanged. TOF-ERDA had shown that under these conditions large fraction of the Na ions diffused out of the sample and evaporated at the surface [9].

The basic mechanism of epitaxial regrowth of ion-irradiated quartz has been discussed by Roccaforte et al. [6–8] using ideas developed by Spaepen, Turnbull, and others [14–17]. It is noteworthy that, in all the cases with implanted alkali ions studied so far, the epitaxy of the amorphized layer, the out-diffusion of the alkali ions, and the oxygen exchange between the SiO_2 matrix and the annealing gas are highly correlated [4, 6]. The most important reaction step consists in binding an implanted alkali ion A to the dangling oxygen ion, which is produced as radiation damage during the implantation of A (or any other ions) [4, 6]. In the presence of migrating oxygen (O^*), this process can be described as

$$O_3{\equiv}Si{-}O{-}Si{\equiv}O_3 + 2A + O^*$$
$$\rightarrow O_3{\equiv}Si{-}O{-}A + A{-}O^*{-}Si{\equiv}O_3$$
$$\rightarrow O_3{\equiv}Si{-}O^{(*)}{-}Si{\equiv}O_3 + A_2O.$$

O^* denotes external ^{18}O and $O^{(*)}$ refers to either ^{18}O or ^{16}O. In both crystalline quartz and amorphous silica, the building blocks are corner-connected tetragons, which we abbreviate as $O_3{\equiv}Si{-}O$. As the A–O bond is energetically weaker (≈3 eV) than the Si–O bond (4.57 eV), annealing disrupts first the A–O bond leading to alkali release and diffusion and then the Si–O bond, which leads to the photoactive E' center ($O{\equiv}Si\bullet$).

3.2 Luminescence spectra at 10 K

The CL spectra and deduced intensities measured at 10 K sample temperature are illustrated in Fig. 2(a) and (b). The spectra are dominated by a rather broad blue band at 2.90 eV, which we did not observe in the room-temperature measurements (see below and [9–11, 18, 19]). Decomposition of these spectra was tried by including the bands at 2.40 and 3.25 eV, which are known to be present at room temperature in this spectral range (see Sect. 3.3). However, it was found that the intensity of the 2.40-eV green band was smaller by two orders of magnitude relative to the 2.90-eV band and therefore was neglected. Furthermore, the intensity of the violet band at 3.25 eV turned out by roughly one order of magnitude weaker than that of the 2.90-eV band as shown

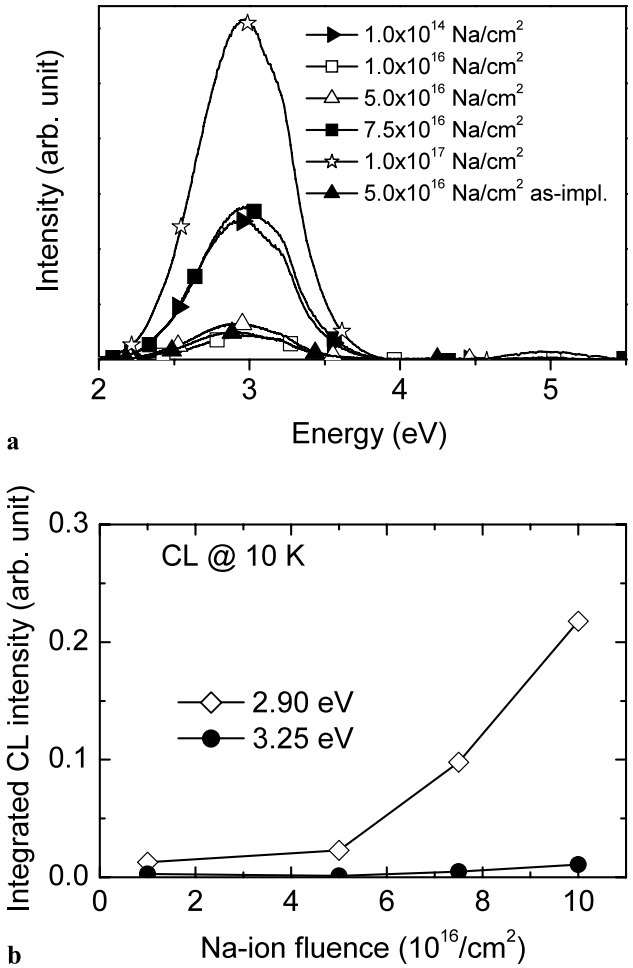

Fig. 2 (**a**) CL spectra taken at 10 K as function of the Na-ion fluence after annealing in $^{18}O_2$-gas at 1123 K. (**b**) Variation of the relative CL intensities at 10 K as function of the Na-ion fluence

in Fig. 2(b). As shown in Fig. 2(b), the 2.90-eV band rises strongly in intensity with the implanted Na fluence and for that reason may be tentatively considered of ion-specific nature. Finally, another broad and rather weak UV peak around 5.0 eV appeared in the spectra (see Fig. 2(a)).

In recent years, various authors have reported on the observation of a 2.9-eV photoluminescence (PL) emission band in amorphous *silica* at room or low temperature [20–22]. Guzzi et al. [20] have measured UV-excited PL spectra of fused silica at 60–300 K. Their spectra exhibit an energy shift of the blue line from 3.1 eV at room temperature to a triplet at 60 K having its main component at 2.7 eV; in addition a strong 4.4-eV peak appears at low temperature. Similarly, room-temperature PL measurements on Ge-doped silica by Anedda et al. [21] exhibit a weak band at 2.90(3) eV having a FWHM of 0.45(5) eV. Finally, Pealari et al. [22] have recently observed a 2.9-eV PL band in silica synthesized by a sol-gel method. This band has a long decay constant of about 800 μs and overlaps with a broader 3.7-eV PL band of 0.78–0.85 eV FWHM. The total intensity of the doublet increases by almost an order of magnitude when decreasing the sample temperature from 300 K to 8 K; the 2.9-eV band appears to be predominant at the PL excitation with 6-eV photons.

We are not aware of any work reporting on the identification of the 2.90-eV band in *α-quartz* during CL or PL spectroscopy at low temperatures, and there are rather few data on the temperature dependence of CL and PL emission in α-quartz after ion, neutron, or γ-ray irradiation [2]. The PL activity of α-quartz after γ-irradiation has been recently measured by Cannas et al. [23, 24] at 17.5–300 K using 7.6-eV photon excitation. These PL spectra gave evidence for two Gaussian-shaped bands, a blue band at 2.7 eV and a UV band at 4.9 eV. Both energies do not depend on the temperature, but the intensities of the bands do and are thermally quenched with activation energies of 68 and 28 meV, respectively. At 17.5 K, the time constants of 3.6 ns and 1.0 ns are definitely much shorter than the μs time constants of the 2.95 and 3.25-eV CL bands measured in α-quartz by Sahoo et al. [25] at room temperature, or the 800-μs time constant of the 2.9/3.7-eV PL doublet found by Pealari et al. [22] in silica. A fast PL band centered around 2.7 eV has also been found in SIMOX structures produced by oxygen ion implantation in silicon [23, 24] and has been attributed to defects at the interface between Si clusters and the SiO_2 matrix.

3.3 Luminescence spectra at 300 K

For comparison, Fig. 3(a) illustrates the CL spectra previously taken at room temperature for the samples irradiated with 10^{14}–10^{17} Na-ions/cm^2 and annealed for 1 h at 1123 K [9]. All these spectra exhibit several broad and narrow peaks, which have been fitted by adopting the CL "fingerprints" of the known intrinsic and alkali-ion specific subbands listed in Table 1 [9–11, 18, 19, 26–31].

The relative intensities of these bands at 300 K are plotted in Fig. 3(b) *versus* the Na-ion fluence. We first note that the intensities of the three "intrinsic" CL bands at 2.40 eV (green), 2.79 eV (blue-violet) and 4.30 eV (UV) generally vary little with the ion fluence. These "intrinsic" bands [10, 11, 18, 19, 26–31] are related to the amorphized or damaged quartz matrix but do not depend on the particular ion species implanted or more generally on the amorphization process. The near-constancy of the intensities of the intrinsic bands can be easily explained by the fact that in all the cases the ion fluence was high enough to create an amorphized layer (see Fig. 1), which upon annealing did not fully recover even for the highest fluences.

On the other hand, the "ion-specific" [18, 19] violet CL bands at 3.25 and 3.65 eV are directly correlated with the implanted alkali ions, and their intensities generally increase with the ion fluence. CL data have been previously taken for

Table 1 CL emission bands observed at RT in Na-implanted α-quartz annealed in oxygen at 1123 K. The numbers in parentheses give the uncertainties

CL band (eV)	Wavelength (nm)	Width (eV)	Defect center
2.40(2)	514(4)	0.16(2)	Non-bridging OH centers (NBOHC)
2.79(3)	442(5)	0.40(5)	ODC and/or E' center
3.25(4)	380(4)	0.44(6)	Neutral oxygen vacancy, charge-compensated alkali-ion center
3.65(3)	338(3)	0.48(8)	Defect related to implanted Na ions
4.30(5)	287(3)	0.58(12)	ODC center

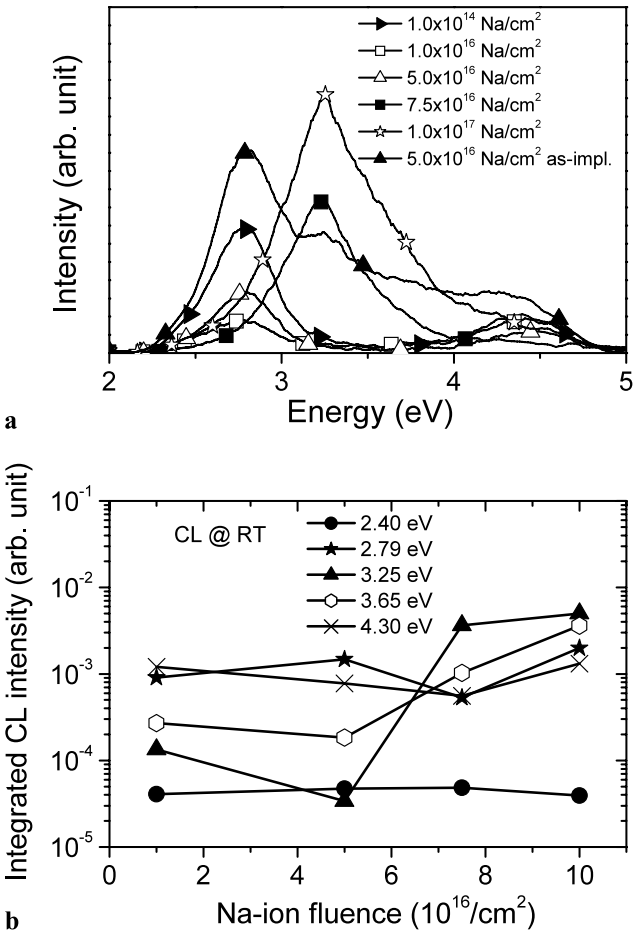

Fig. 3 (**a**) Room-temperature CL spectra of α-quartz samples irradiated to fluences of 1×10^{14}–1×10^{17} Na-ions/cm^2 and annealed for 1 h in $^{18}O_2$-gas at 1123 K. An as-implanted CL spectrum for 5×10^{16} Na-ions/cm^2 is also given. (**b**) Variation of the relative CL intensities at 300 K as function of the Na-ion fluence

a fixed Na fluence of 2.5×10^{16}/cm^2 as function of the annealing temperature [9]. Under these conditions, the intensity of the 3.65-eV band directly correlates with the fraction of Na retained in the SiO_2 matrix, which of course decreases for increasing annealing temperature, due to alkali ion out-diffusion. On the other hand, the intensity of the 3.25-eV band appears to reflect the degree of epitaxy: it decreases after full epitaxy at the highest temperature was achieved. For a more detailed discussion of the ion-specific bands in α-quartz, see [9–11, 18, 19].

The emission of visible and UV luminescence light of α-quartz after ion and electron bombardment is quite a complicated process, and for that reason the assignment of photoactive defect structures must be still considered rather tentative. According to Stevens-Kalceff [26–28] and Skuja et al. [29–31], the 2.79-eV and 4.30-eV bands are associated with oxygen-deficiency centers (ODC, $O_3{\equiv}Si–Si{\equiv}O_3$) or their precursors produced during ion-irradiation. The peak at 2.40 eV was connected either to oxygen vacancy-interstitial pairs (V_o; $(O_2C)_i$) or to irradiation-induced self-trapped excitons (STE) within the a-SiO_2 outgrowth at the top of the sample containing a large number of peroxy linkages (≡Si–O–O–Si≡). More recently, the 2.40-eV band was confirmed to originate from the electron bombardment of virgin α-quartz during the CL measurements [10, 11]. The 3.65-eV band is intimately related to the $O_3{\equiv}Si–O–A$ structure mentioned before, while the 3.25-eV again appears to be related to a $O_3{\equiv}Si–Si{\equiv}O_3$ (ODC) configuration [10, 11, 29–31].

4 Conclusions

The present experiments provide a successful attempt at monitoring cathodolumi-nescence during *chemical* epitaxy of α-quartz after Na-ion implantation. We demonstrated that the degree of epitaxy achieved at the fixed temperature of 1123 K and the CL spectra strongly depend on the implanted Na ion fluence. For the first time, systematic CL spectra were taken at 10 K sample temperature, as a function of the implanted Na ion fluence and after annealing the irradiated samples in $^{18}O_2$ gas at 1123 K. The shapes of the CL spectra vary little with the ion fluence, with a broad 2.90-eV band dominating and its intensity rising almost proportionally to the fluence. More information on the luminescence mechanism, local environment, and possible nano-particle formation is necessary to unambiguously correlate the CL bands with the defect structures, especially those responsible for the low-temperature emission. A classification of the light emitting defects in α-quartz has been recently presented by Keinonen et al. [33]. Besides the point defects mentioned

before, these authors also discuss the properties of Si nanoclusters embedded in silica based on Molecular Dynamics simulations.

At room temperature, besides the intrinsic CL bands at 2.40, 2.79, and 4.30 eV, there exist two strong bands in the blue-violet region (3.25 and 3.65 eV). Their intensities appear correlated in a characteristic way with the Na outdiffusion and epitaxy of the matrix. Bands at the same photon energies and with similar features have also been observed during *chemical* epitaxy after Rb [10, 11] or double Rb/Ge ion implantation [25] and after *excimer-laser* treatment of Rb- or Cs-doped quartz [5].

Acknowledgements The authors would like to thank Dr. L. Ziegeler for his help with the $^{18}O_2$ annealing experiments, Professor H. Hofsäss for helpful comments, and D. Purschke for skillfully operating the IONAS implanter. This work has been supported by the Deutsche Forschungsgemeinschaft (DFG).

References

1. E. Lell, H.J. Kreidl, J.R. Hensler, *Radiation Effects in Quartz, Silica and Glasses* (Pergamon, New York, 1996)
2. R.A.B. Devine, J.-P. Duraud, E. Dooryhee (eds.), *Structure and Imperfections in Amorphous and Crystalline Silicon Dioxide* (Wiley, New York, 2000)
3. L. Rebohle, J. von Borany, H. Fröb, W. Skorupa, Appl. Phys. B **70**, 131 (2000)
4. K.P. Lieb, in *Encyclopedia of Nanoscience and Nanotechnology*, ed. by H.S. Nalwa, vol. 3 (Am. Scient. Publ., Stevenson Ranch, 2004), pp. 233–251
5. P.K. Sahoo, S. Gąsiorek, S. Dhar, K.P. Lieb, P. Schaaf, Appl. Surf. Sci. **252**, 4477 (2005)
6. F. Roccaforte, W. Bolse, K.P. Lieb, Appl. Phys. Lett. **73**, 1349 (1998)
7. F. Roccaforte, W. Bolse, K.P. Lieb, J. Appl. Phys. **89**, 3611 (2000)
8. F. Roccaforte, F. Harbsmeier, S. Dhar, K.P. Lieb, Appl. Phys. Lett. **76**, 3709 (2000)
9. S. Gąsiorek, P.K. Sahoo, S. Dhar, K.P. Lieb, T. Sajavaara, J. Keinonen, J. Non-Cryst. Solids **352**, 2986 (2006)
10. J. Keinonen, S. Gąsiorek, P.K. Sahoo, S. Dhar, K.P. Lieb, Appl. Phys. Lett. **88**, 261102 (2006)
11. S. Gąsiorek, P.K. Sahoo, S. Dhar, K.P. Lieb, K. Arstila, J. Keinonen, Appl. Phys. B **84**, 357 (2006)
12. M. Uhrmacher, K. Pampus, F.J. Bergmeister, D. Purschke, K.P. Lieb, Nucl. Instrum. Methods B **9**, 234 (1985)
13. J.F. Ziegler, J.P. Biersack, *Computer program SRIM2000*, http://www.srim.org/
14. F. Spaepen, D. Turnbull, AIP Conf. Proc. **50**, 73 (1979)
15. V.J. Fratello, J.F. Hays, F. Spaepen, D. Turnbull, J. Appl. Phys. **51**, 6160 (1980)
16. P.K. Gupta, A.R. Cooper, J. Non-Cryst. Solids **123**, 14 (1990)
17. L.W. Hobbs, A.N. Sreeram, C.E. Jesurum, B.A. Berger, Nucl. Instrum. Methods B **116**, 18 (1996)
18. K.P. Lieb, J. Keinonen, Contemp. Phys. **47**, 305 (2006)
19. K.P. Lieb, P.K. Sahoo, S. Gąsiorek, S. Dhar, J. Keinonen, Physica B **389**, 9 (2007)
20. M. Guzzi, M. Martini, M. Mattaini, F. Pio, G. Spinolo, Phys. Rev. B **35**, 9407 (1987)
21. A. Anedda, C.M. Carbonaro, F. Clemente, R. Corpino, A. Serpi, J. Non-Cryst. Solids **315**, 161 (2003)
22. A. Paleari, N. Chiodini, D. Di Martino, F. Meinardi, Phys. Rev. B **71**, 075101 (2005)
23. H. Nishikawa, R.E. Stahlbusch, J.H. Stathis, Phys. Rev. B **60**, 15910 (1999)
24. M. Cannas et al., J. Phys. Condens. Matter **16**, 1731 (2004)
25. P.K. Sahoo, S. Gąsiorek, K.P. Lieb, K. Arstila, J. Keinonen, Appl. Phys. Lett. **87**, 021105 (2005)
26. M.A. Stevens-Kalceff, Phys. Rev. B **57**, 5674 (1998)
27. M.A. Stevens-Kalceff, Phys. Rev. Lett. **88**, 3137 (2000)
28. M.A. Stevens-Kalceff, J. Wong, J. Appl. Phys. **97**, 113519 (2005)
29. L.N. Skuja, A.N. Trukhin, Phys. Rev. B **39**, 3409 (1989)
30. L.N. Skuja, J. Non-Cryst. Solids **239**, 16 (1998)
31. L.N. Skuja, A.R. Silin, A.G. Boganov, Phys. Rev. B **58**, 14296 (1998)
32. A. Cannizzo, S. Agnello, S. Grandi, M. Leone, A. Magistris, V.A. Radzig, J. Non-Cryst. Solids **351**, 1805 (2005)
33. J. Keinonen, F. Djurabekova, K. Nordlund, K.P. Lieb, in *Silicon Nanophotonics*, ed. by L. Khriachtchev (World Scientific, Singapore, 2008), p. 379, Chap. 14